Polymer Journal (2021) 53:81–91
https://doi.org/10.1038/s41428-020-00426-2

REVIEW

The cyanobacterial polysaccharide sacran: characteristics, structures, and preparation of LC gels

Kosuke Okeyoshi[1] · Maiko K. Okajima[1] · Tatsuo Kaneko[1]

Received: 2 July 2020 / Revised: 9 September 2020 / Accepted: 9 September 2020 / Published online: 6 October 2020
© The Society of Polymer Science, Japan 2020

Abstract

To shift from a petroleum-dependent society to a sustainable society using eco-friendly materials, polysaccharides from natural products are important candidates as alternative materials. We have researched one cyanobacterial polysaccharide, "sacran", which is extracted from *Aphanothece sacrum*. In this review, the unique characteristics and structures of sacran and the preparation of liquid crystal gels are introduced: polymer properties such as megamolecular weight, that is, a weight > 10^7 g/mol; characteristic viscosity; liquid crystallinity (LC); fiber structures on the nanometer/micrometer scale; gel formation with heavy metal ions; photoshrinking in gels composed of metal ions; anisotropically swelling gels; orientation upon drying of the air-LC interface; meniscus splitting; and membrane formation with uniaxial orientation, which are the results of self-organization. These matters are discussed particularly from the perspectives of polymer science, colloidal science, gel science, etc. We expect that sacran will be applicable in a variety of fields, such as tissue engineering, pharmacodynamics, and biomedical materials, with possible contributions to the development of a sustainable material society.

Introduction

The twenty-first century may be an important period for shifting from a petroleum-dependent society for both materials and energy to a sustainable society using biomaterials. In fact, we are experiencing environmental problems such as substantial global warming and microplastics pollution. Therefore, the activities of plants, such as carbon fixation through photosynthesis, have been studied. One of the expected technologies is capturing carbon dioxide and utilizing it for the preparation of renewable sources such as methane and formic acid. The utilization of natural products such as polysaccharides is an important strategy to solve these problems by using petroleum-based plastics. With this background, many researchers have studied various kinds of saccharides and polysaccharides to construct a sustainable society [1–12]. In fact, because they are thin, lightweight, and tough, some kinds of polysaccharides, such as cellulose nanofibers from timbers and chitin/chitosan from crustaceans, have been widely studied as alternative materials for synthesized plastics used in automobile parts, cosmetic products, etc. Pullulan, a polysaccharide, has been studied as an advanced medical material for utilization in drug transportation systems [13, 14]. By using the self-assembled nanogel structure as a molecular chaperone, it has a considerable potential to transport proteins to target locations. Water-soluble polysaccharides, in particular, show a unique structural hierarchy due to the varieties of functional groups on the side chains, the network topology, the molecular weight, etc.

Aphanothece sacrum [15] is a freshwater unicellular cyanobacterium that efficiently fixes CO_2 during aquacultivation in rivers (Fig. 1a). It has many exopolysaccharides as an extracellular matrix with a high water content of ~97.5% [16–18]. The polysaccharides are extracted by using an alkaline aqueous solution (0.1 N sodium hydroxide), with yields of more than 50 wt% on the gram scale. By infrared absorption spectrometry and X-ray photoelectron spectroscopy (XPS), it has been demonstrated that the polysaccharides have sulfated groups. The sulfation degree is ~10 mol% for monosaccharide units, as determined through XPS analysis and CHNS elemental analyses. The polysaccharide is

✉ Tatsuo Kaneko
kaneko@jaist.ac.jp

[1] Japan Advanced Institute of Science and Technology, 1-1 Asahidai, Nomi, Ishikawa 923-1292, Japan

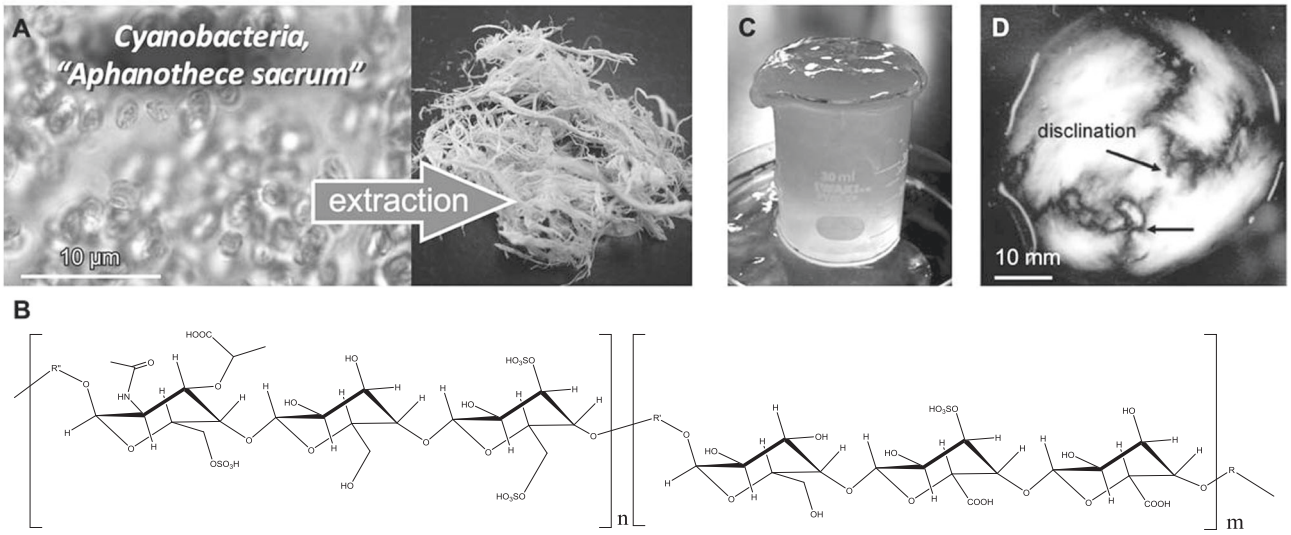

Fig. 1 Cyanobacterial polysaccharides, sacran. **a** Microscopic images of cyanobacteria, *Aphanothece sacrum*, and the extracted polysaccharides, sacran. **b** Partial chemical structure of sacran. **c** Super water-absorbent nature of sacran. **d** Images of a sacran solution under crossed Nicols polarimetry. Polymer concentration: 0.5 wt%. Copyrights: partially reproduced from [18] and [20]

composed of various monosaccharide units, e.g., glucose, galactose, mannose, xylose, rhamnose, and fucose, with compositions of 25.9%, 11.0%, 10.0%, 16.2%, 10.2%, and 6.9%, respectively. Additionally, it has 20–25% uronic acids and ~1% arabinose, galactosamine, and muramic acid. The main chemical structure is partially determined by fragment analysis through Fourier transform ion cyclotron resonance mass spectrometry (Fig. 1b). These analytical studies revealed that the polysaccharide is a new polymer, which we named "sacran."

In this review, the unique characteristics, structures, and preparation of sacran liquid crystallinity (LC) gels are introduced [16–40]. One of the unique characteristics of sacrans is that aqueous solutions show super water retentivity (Fig. 1c). Generally, it is difficult to dissolve polymers with ultrahigh molecular weights in water due to the effects of strong segregation [41]. However, sacran exhibits water solubility despite its ultrahigh molecular weight, which promises unique properties. Although physically cross-linked sacrans show gel-like stability in the stationary state, they convert to a dispersed state upon vigorous agitation. In addition, upon irradiation with cross-polarized light (Fig. 1d), the aqueous solution shows LC at a low concentration of ~0.5 wt%. Starting with these unique characteristics, we introduce polymer properties such as molecular weight, viscoelasticity, morphology, absorbance of heavy metal ions, self-assembly, self-organization, and anisotropic characteristics of hydrogels. Considering recent environmental problems, such as global warming and microplastics pollution, polymer materials obtained from natural products, such as cyanobacterial polysaccharides, are expected to be excellent alternatives to petroleum-derived plastics in the development of a sustainable society.

Polymer properties

Molecular weight

The absolute molecular weight of sacran, M_w, measured by using multiangle static light scattering (MALLS) was $>10^7$ g/mol [23]. When sacran was detected by RI and LLS after 13 min of flowing, the concentration was low enough to regard it as a solution of an elementary sacran (Fig. 2a). Additionally, a typical Zimm–Berry plot was obtained (Fig. 2b) [21]. The M_w was estimated to be 2.4×10^7 g/mol, the radius of gyration R_g was 402 nm, and the second virial coefficient, A_2, was 4.5×10^{-4} mol cm^3/g^2. By repeating the extraction under different elution conditions, such as different alkaline concentrations, the elution times, rates of agitation, and solvents for reprecipitation, it was concluded that the M_w determined from the MALLS measurement ranged from $1–3 \times 10^7$ g/mol. This value suggested that sacran is a giant polymer.

Viscosity

The viscosity of aqueous solutions of sacran under a variety of concentrations was investigated to study the critical concentration of liquid crystallization [22, 23]. Figure 3a shows the shear rate dependence of the rotation viscosity of the aqueous sacran solutions. The zero-shear viscosity was estimated through extrapolation at a shear rate range of 10^{-3}–10^{-2} s^{-1}. The viscosity also increased with an increase in concentration. However, an inflection point was observed around a polymer concentration of 0.25–0.5 wt%. To clarify the relation of the inflection point and the liquid crystallization of the aqueous solutions, polarimetry was

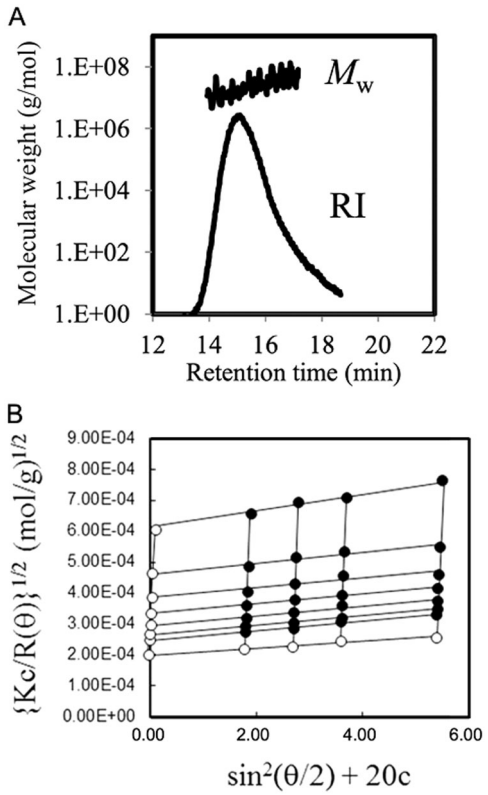

Fig. 2 Molecular weight of sacran. **a** Absolute weight-average molecular weight, M_w, of sacran, determined by multiangle static laser light scattering (MALLS). **b** Zimm–Berry plots for determination of molecular weight. Copyrights: partially reproduced from [21] and [23]

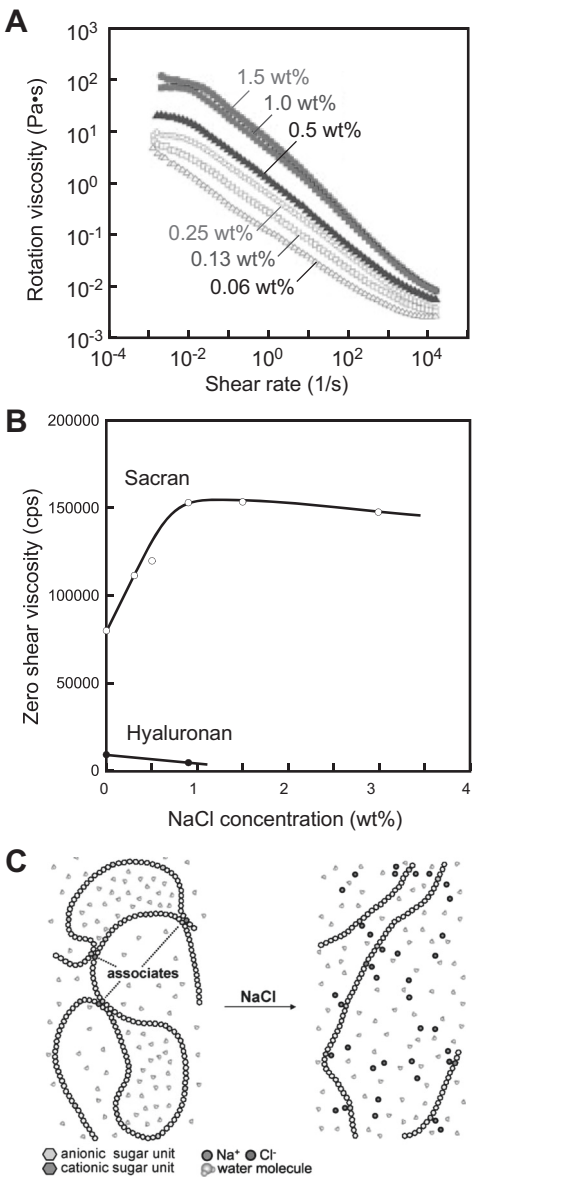

Fig. 3 Viscosity of sacran and nanostructure transformation of sacran chains. **a** Shear rate dependence of apparent viscosity for solutions at 25 °C. **b** Changes in the zero-shear viscosity of sacran and hyaluronan in NaCl solution. **c** Schematic illustration of nanostructure transformation of sacran chains. Sacran forms nanoloops through electrostatic interactions of cationic units with anionic units. The nanoloop structures effectively retain water molecules. Salt addition breaks nanoloop interaction points into longer chains several micrometers in length, maintaining the high retention capacity of water. Copyrights: partially reproduced from [17] and [18]

also investigated by observation with crossed Nicols. From the analysis, we concluded that the critical concentration of liquid crystallization was 0.25–0.5 wt%.

As shown in Fig. 3b, the rotation viscosity measurement for the 1 wt% solution showed a remarkably high zero-shear viscosity of 83,000 cP, while the hyaluronic acid with a lower M_w ~150–180 kDa showed a value of 8900 cP. This remarkable difference was attributed to the M_w difference. To clarify the polymeric chain interaction, the effect of the presence of salt was investigated. The addition of 0.9% NaCl to the hyaluronic acid solution resulted in a decrease in the viscosity to approximately 4400 cP. This was attributed to the charge screening effects of salts [42]. However, the viscosity of the sacran sol increased to ~153,000 cP. Since sacran should have semirigid rod structures similar to other kinds of natural polysaccharides [43], they may recover their extended conformation as a result of the disruption of electrostatic interactions. One hypothesis is that the small decrease in the sacran sample should be related to the salt-induced transformation by extending the chains to the micrometer scale in length. Although the addition of salt could break the nanoloop structures to attenuate the absorbability of water, it should contribute to the increase in hydration by extending the polymer chains (Fig. 3c).

Polymer self-assembly

Fiber formation

From the dielectric behaviors of sacran solutions, structural changes are discussed as a function of the polymer concentration (Fig. 4a) [18]. Dielectric relaxation studies indicated that the critical concentration, c^*, was 0.02 wt%.

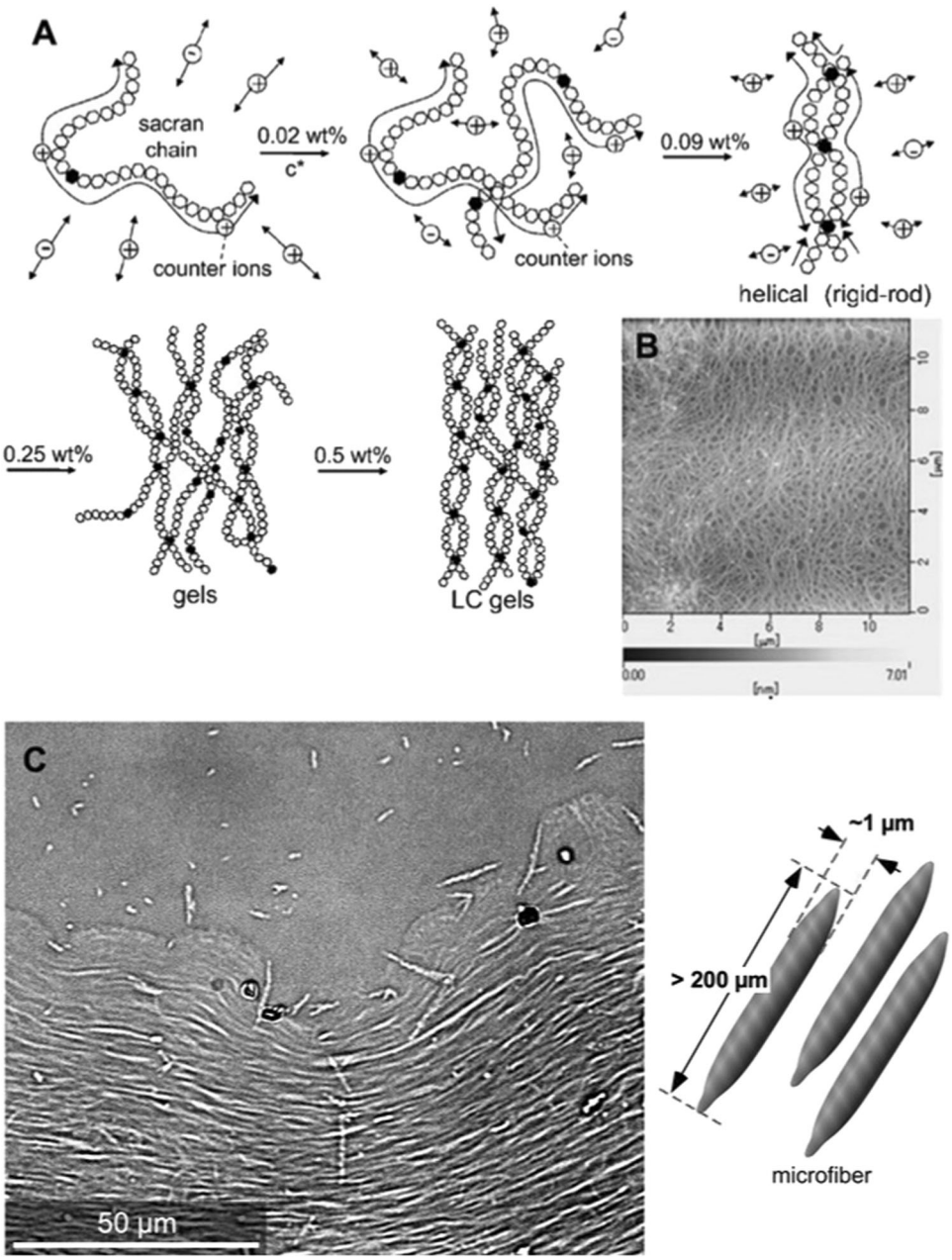

Fig. 4 Fiber structures of sacran from the molecular scale to the micrometer scale. **a** Schematic of molecular behaviors in the sacran chain as the concentration increased. The + and − symbols indicate counter cations and anions in the polymer chain, respectively. Black marks on chains indicate amino monosaccharide units. The lengths of arrows along the chain indicate fluctuation lengths. **b** AFM image of the dried sample on a mica substrate. **c** Optical microscopy images of the dried sample cast from the 0.5 wt% aqueous solution onto a glass substrate. Schematic illustration of the sacran microdomain. Copyrights: partially reproduced from [18], [21], and [25]

In the range of concentrations between 0.02 and 0.09 wt%, sacran chains have many opportunities to overlap each other but do not show associations. When the concentration is more than 0.09 wt%, sacran chains form double helical and rigid structures. At 0.25 wt%, the aqueous sacran solution shows a sol–gel critical state phase because of an increase in chain entanglement and the fraction. The nematic LC phase seems to form at ~0.5 wt%. The cast sample from the aqueous solution was observed by AFM in dynamic force modulation mode (Fig. 4b) [21]. It is possible to imagine that the polymer network is composed of long sacran ropes.

Furthermore, we observed microfibers with diameters of ~1 μm and lengths of >200 μm by optical microscopy (Fig. 4c) [25]. This is a result of self-assembly in water, and they easily orient on a drying interface. In contrast to other polysaccharides, such as cellulose, which show needle-like crystals with lengths of 1 μm or less [44–46], the sacran microfiber has a remarkably large self-assembled structure. The microfiber also disassembles into fiber bundles ~50 nm in diameter by adding anionic surfactants such as sodium dodecyl sulfate [31].

LC gel formation

When sacran solutions were dropped in an aqueous In^{3+} solution, they formed gel beads [19]. After the addition of the

aqueous sacran solution, those with concentrations of >0.33% formed gel beads as a result of binding In^{3+}. In addition, as seen in Fig. 5a, observation under crossed Nicol polarimetry clearly confirmed the birefringence of the gel samples in aqueous solutions of >0.25%. Similarly, gel formation was confirmed in both sacrans with Yb^{3+} and alginates with Yb^{3+} (Fig. 5b). Notably, sacran could form beads in the presence of Yb^{3+} under both acid and alkaline conditions, but alginates under acidic conditions formed no gel beads. The beads were formed more effectively upon metal binding under acidic conditions. This result of the sacran sample might be due to the existence of sulfate groups in the sacran chain. Heavy metal ions having N electron orbitals exhibit a variety of coordination types, suitable for sacrans containing nine or more sugar units, e.g., uronic acid, muramic acid, and mannose with vicinal hydroxyl groups. Considering that trivalent metal ions contain rare metals, this demonstration using sacran may allow innovative methods for the pretreatment of waste solutions for metal recovery.

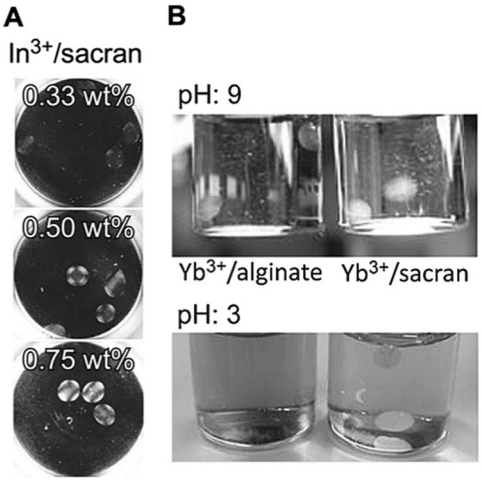

Fig. 5 LC gel formation with heavy metal ions. **a** Photoimages of the formation of gel beads by dropping aqueous sacran solutions into a 10^{-2} M indium trichloride aqueous solution, taken under crossed Nicols. **b** Photoimages of the formation of gel beads by dropping sacran or alginate aqueous solutions into alkaline and acid solutions. Concentration of $YbCl_3$: 10^{-2} M. Copyright: partially reproduced from [19]

Sacran/metal composites exhibited hydrophobization and insolubilization in response to ultraviolet light irradiation [20]. The mechanism was verified by checking the gel formation in a mixture of metal ions and sacran or alginate in aqueous solutions. Exploiting this quality, the effect of UV irradiation on the volume change of these gels was evaluated. For the metal ions, we chose the trivalent ions, expecting gelation as a result of mixing. Each aqueous polymer solution was dropped into each metal ion solution to form gel beads. As an example (Fig. 6a), the alginate/Eu^{3+} gel showed deformation at an irradiation energy of 23 J cm^{-2} and deterioration at 46 J cm^{-2}. At energies > 280 J cm^{-2}, the gel primarily shrank and completely disappeared at 530 J cm^{-2}. Whereas the alginate samples showed degradation by UV irradiation, the

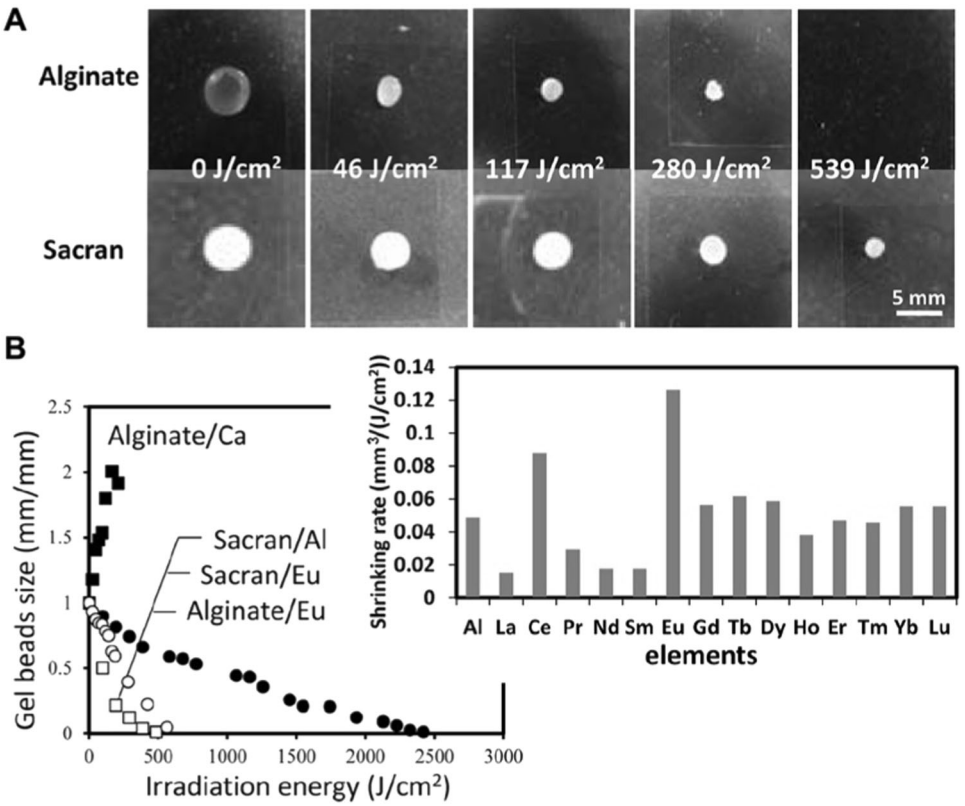

Fig. 6 Photoshrinking of polysaccharide gels interacting with trivalent metal ions. **a** Images of photoshrinking of alginate/Eu^{3+} and sacran/Eu^{3+} gels. **b** Effect of UV irradiation on the size change of alginate/Eu^{3+} gel and sacran/Eu^{3+} gel beads. Wavelength of UV light: 250−450 nm. Inset: shrinking speed of sacran gel beads with a variety of trivalent metal ions. The shrinking speed was estimated from the initial slope of the main figure. Copyright: partially reproduced from [20]

sacran/Eu^{3+} gel gradually shrank without deterioration. Thus, unlike the degradation of alginate/metal composite gels, the sacran/metal gel samples gradually shrank depending on the irradiation energy. UV-induced shrinking of the sacran/metal gels should occur because of the hydrophobization of uronic acid on the basis of photodecarboxylation.

To quantify the gel volume, the size of the gel at each irradiation energy was evaluated. The sacran/Eu^{3+} gel shrank at a speed of 0.13 $mm^3/(J/cm^2)$, corresponding to 22 $mm^3\ h^{-1}$, whereas the shrinking rate of the alginate/Eu^{3+} gel was 0.36 $mm^3/(J/cm^2)$. This difference means that the rate of volume change of the alginate/Eu^{3+} gel was approximately three times faster than that of the sacran/Eu^{3+} gel due to the effective photolysis in the alginate samples (Fig. 6b). When divalent calcium ions were added, the alginate gel swelled upon photoirradiation. This was attributed to the electrostatic interaction among alginates and the weaker nature of Ca^{2+} than that of alginates and Eu^{3+} during photolysis. In contrast, compared with the sacran/Eu^{3+} gels, the sacran/Al^{3+} gels exhibited gradual shrinking. The shrinking speed of the sacran-composited gels with a variety of trivalent ions was calculated (Fig. 6b, inset). When metal electrons are in the photoexcited state and relax back to the ground state, carboxylate radicals should be generated because of metallic free radical formation. This photoshrinking is expected to occur in a mixture with other trivalent ions. It is expected that, by using the composites, controlled release will be useful in targeted cancer therapies [47] and virus infection controls [48].

Interfacial orientation and anisotropy

Fiber orientation on an evaporative interface

It is possible to use an evaporative interface for the polymeric orientation to prepare a film with an ordered structure. Focusing on the drying process of sacran from the LC state, the evaporative interface was analyzed and provided to understand the reconstruction. Differing from most analyses on the LC in the bulk [49, 50], we examined the dynamics of the microdomains on the evaporative interface by monitoring the changes in orientation in the lateral view of the cell. The LC dynamics and the interface effect on the polymer deposition were evaluated by examining how the microdomains' mobility was affected by the domain size, molecular weight, polymer concentration, and drying temperature. Figure 7a shows that the sacran solution in the drying process was observed with a polarized light microscope with a first-order retardation plate. Notably, the solution had a single macrodomain on the air-LC interface. This observation suggests that the microrods as the microdomain orient and integrate parallel to the meniscus curve.

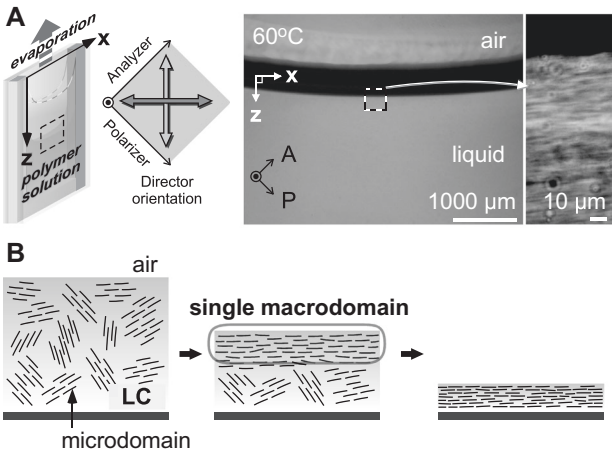

Fig. 7 Milliscale self-integration of sacran on a drying air-LC interface. **a** Polarized microscopic image of sacran solution in a cell with a 1 mm gap after 6 h of drying at 60 °C. The image was taken through crossed Nicols with a first-order retardation plate, $\lambda = 530$ nm. **b** Schematic of microdomain mobility during drying. Microdomains with low mobility show a stable LC state and orient to form a single macrodomain from the evaporative air-LC interface. Copyrights: partially reproduced from [25]

By using an LC polymer with low mobility, such as sacran, in drying, it was possible to order the microdomain on the interface into a single macrodomain (Fig. 7b).

Anisotropic structures

Focusing on the liquid crystallinity, LC gels were prepared by introducing physical or chemical cross-linking points [23, 24, 27, 29]. Specifically, in-plane-oriented films were obtained by drying the LC aqueous solutions at a temperature of 60 °C. The films were annealed at temperatures in the range of 70–140 °C, and they demonstrated in situ hydrogelation to form anisotropic hydrogels. In fact, the films showed a maximum of 70-fold swelling, more in thickness than in width (Fig. 8a). Moreover, the degree of orientation of films in the plane direction was estimated to be $f = 0.46$ from an image obtained by wide-angle X-ray diffraction, comparable with the typical value of nematic solutions. As seen from SEM observation, the film has a layered structure parallel to the evaporative interface (Fig. 8b). This structure induces unidirectional swelling of the gel, seemingly with absorbing water from the side and remarkable swelling in the thickness direction (Fig. 8c).

Furthermore, it was possible to fix the layered structures by a freeze-drying process, and micropores were generated due to the sublimation of water microcrystals. The micropores were apparently interconnected during the process, similar to tunnels in the internal structure of the hydrogels [35]. On the other hand, chemically cross-linked gels with layered structures were also prepared by using divinyl sulfone among carboxyl groups in sacran chain [24]. Thus, the LC characteristics of sacran allowed the preparation of

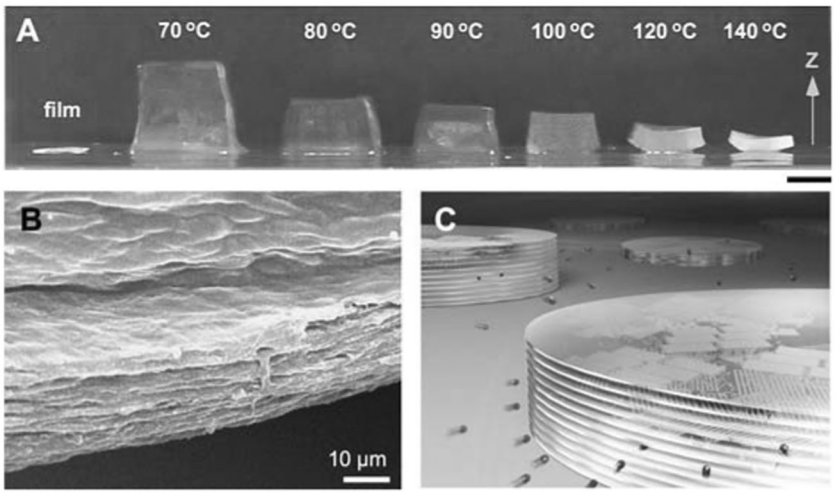

Fig. 8 Anisotropic swelling in sacran hydrogels with layered structures. **a** Sacran film and sacran hydrogel swelling after annealing the film at a variety of temperatures. **b** SEM image of the film in a cross-sectional view. **c** Schematic illustration of a hydrogel with a layered structure that enables directional control for diffusion and swelling. Copyrights: partially reproduced from [23], [27], and [29]

hydrogels with anisotropic structure and swelling. By utilizing the gel's characteristics, the hydrogels are expected to be useful for many applications: drug carriers [51–53], catalyst adsorbents [54, 55], filters [56, 57], etc.

Uniaxial orientation through meniscus splitting

By using the evaporative interface in a limited space, one dissipative structure is introduced [28, 31, 34]. The sample was filled in a top-open cell with a 1 mm gap. By drying a 0.5 wt% sacran aqueous solution at 60 °C, the polymer deposited at specific points bridged the gap to form a membrane in the depth direction (Fig. 9a). The mechanism is as follows (Fig. 9b): (1) immediately after deposition nucleation on the interface, which bridges the gap, the capillary force allows the self-integration of the microrods along the interfacial contact line. (2) After nucleation at specific points, the sacran microrod integrates parallel to the contact line to make a membrane with uniaxial orientation.

From a cell with 7 mm width in the *X*-direction, the polymer deposited with only adsorption on the solid surfaces of the cell but no vertical membrane formation. Furthermore, one vertical membrane was formed in the cell with a width of 15 mm, and two were formed in the cell with a width of 21 mm. These numerical differences mean that the mixture experiences interfacial instability during drying, which causes the formation of multiple nuclei. In addition, by checking the case of a wider width, e.g., 100 mm, multiple split menisci and membrane formation were clearly confirmed with a characteristic interval (7–15 mm). This value is strongly associated with the characteristic length in patterns of viscous fingering [58].

Uniaxial swelling in gels

By regulating the geometric conditions for the evaporative interface, we could obtain a dried film from the planar

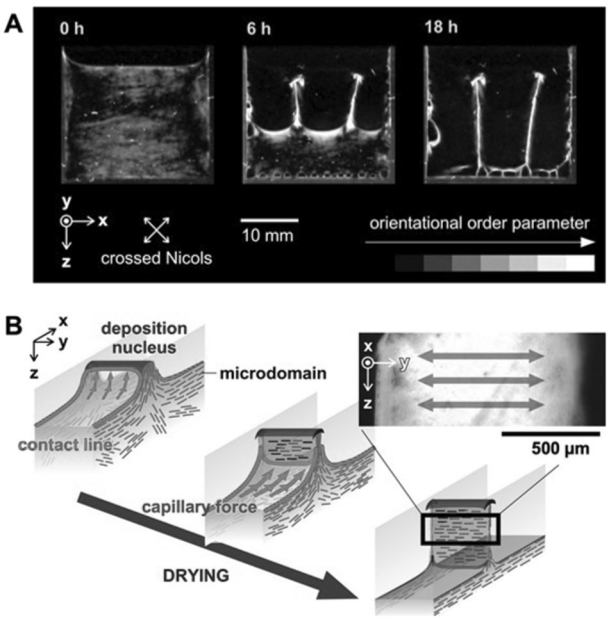

Fig. 9 Meniscus splitting with vertical membrane formation. **a** Images of drying-induced meniscus splitting and vertical membrane formation from a top-open cell (*X*-width, *Y*-thickness, *Z*-depth) = (21, 1, ~20 mm). Initial sacran concentration: 0.5 wt%. Drying temperature: 60 °C. **b** Schematic illustration of vertical membrane formation bridging a gap and orientation of the microrod along the contact line. Copyright: partially reproduced from [28]

interface and a dried membrane from the quasi-linear interface (Fig. 10). By using an annealing technique to introduce cross-linking points, physically cross-linked polymer networks were prepared in both cases. The wetting process was observed by adding water to the dried samples. It was demonstrated that the film showed uniaxial swelling with a $\Delta z_{wet}/\Delta z_{dry}$ of ~50 times [23]. In addition, the stable plain-orientation structure was confirmed in the wet state through cross-polarized light [25, 29]. During swelling, the hydrogel has a stable layered structure for

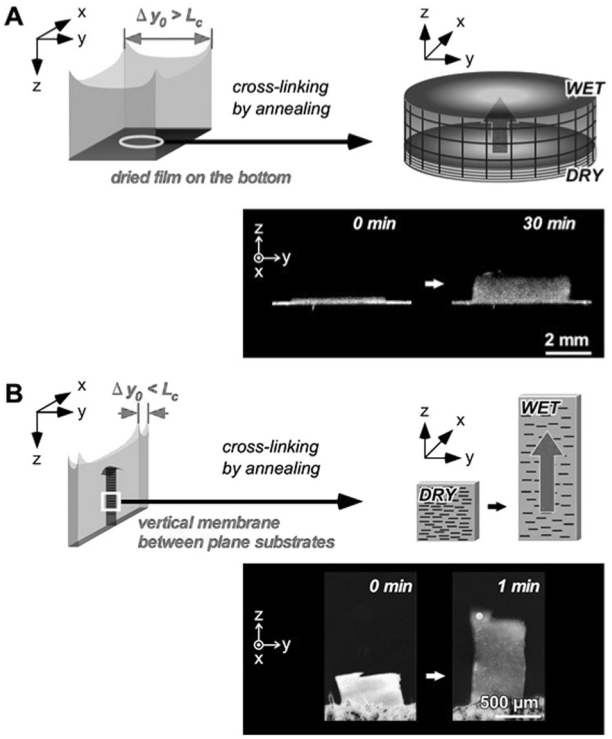

Fig. 10 Two types of uniaxially swelling hydrogels. **a** 3D schematics of the planar evaporation front and linear evaporation front of sacran solutions. **b** Schematics and images of anisotropically swelling sacran hydrogels observed under crossed Nicols. Copyrights: partially reproduced from [28] and [29]

adsorbing water with directional controllability. In addition, the cross-linked membrane exhibited fast uniaxial swelling by approximately four times and maintained the oriented structure [28]. This uniaxial swelling indicates an expansion of the interval on the short axis of the microrods. Swelling is a kind of quasi-1D hydrogel that is potentially useful as a soft actuator with biocompatibility and fast responses of swelling to water absorption or other molecules.

Conclusion and future perspectives

In this review, the cyanobacterial polysaccharide sacran produced by *Aphanothece sacrum* with fixing C and N in H_2O under solar energy was introduced, showing the unique characteristics and design of advanced materials that smartly respond to changes in outer environments. It has megamolecular weight, $>10^7$ g/mol, remarkably large in comparison with other polysaccharides such as hyaluronan. Additionally, the polysaccharide aqueous solution provides unique properties: water retention, liquid crystallinity, and thixotropic viscosity. Because sacrans have hierarchical structures upon self-assembly into fiber structures, we could observe nanofibers with a diameter of ~50 nm and microfibers with a diameter of ~1 μm, which are remarkably large in comparison with others, such as cellulose nanofibers. We also demonstrated that the sacran could form a network with liquid crystallinity in the presence of metal multivalent cations, differing from the presence of monovalent ions such as Na^+.

Furthermore, sacran in aqueous solution also has a periodic nanostructure, which was clarified by the synchrotron X-ray scattering method [59]. The microdomains have also been observed by utilizing optical second-harmonic-generation microscopy [60], where they showed sufficiently high second-order nonlinear susceptibilities. For the preparation of advanced biomaterials, various approaches have been developed by demonstrating cell scaffolds [36], anti-inflammatory [61], anti-allergic effects on the human body, etc. [62–65]. We hope that sacran will be used in a variety of fields, such as tissue engineering, pharmacodynamics, and biomedical materials, contributing to sustainability in low-carbon society.

Acknowledgements The authors sincerely appreciate the great efforts of Dr. Kittima Amornwachirabodee, Dr. Saranyoo Sornkamnerd, Dr. Gargi Joshi, and Ph.D. students. The authors gratefully acknowledge Green Science Material, Inc. (Kumamoto, Japan), Kisendou Corporation (Asakura, Japan), and Kawatake Ganso Endo Kanagawado G.K. (Asakura, Japan) for gifting *Aphanothece sacrum* biomaterials. The research was financially supported by a Grant-in-Aid from A-step, (AS2915173U) of JST, Japan, and a Grant-in-Aid for Scientific Research on Innovative Areas (JP20H05213) from the Ministry of Education, Culture, Sports, Science, and Technology of Japan.

Compliance with ethical standards

Conflict of interest The authors declare that they have no conflict of interest.

Publisher's note Springer Nature remains neutral with regard to jurisdictional claims in published maps and institutional affiliations.

References

1. Marchesault RH, Morehead FF, Walter NM. Liquid crystal systems from fibrillar polysaccharides. Nature. 1959;184:632–3.
2. Holzwarth G, Prestridge EB. Multistranded helix in xanthan polysaccharide. Science. 1977;197:757–9.
3. Fratzl P, Weinkamer R. Nature's hierarchical materials. Prog Mater Sci. 2007;52:1263–334.
4. Lin N, Huang J, Dufresne A. Preparation, properties and applications of polysaccharidenanocrystals in advanced functional nanomaterials: a review. Nanoscale. 2012;4:3274.
5. Zhang R, Edgar KJ. Properties, chemistry, applications of the bioactive polysaccharide curdlan. Biomacromolecules. 2014;15:1079.
6. Ifuku S, Nogi M, Abe K, Yoshioka M, Morimoto M, Saimoto H, et al. Preparation of chitin nanofibers with a uniform width as alpha-chitin from crab shells. Biomacromolecules. 2009;10:1584–8.
7. Kumagai H, Matsunaga R, Nishimura T, Yamamoto Y, Oaki Y, Inoue H, et al. CaCO3/chitin hybrids: effects of recombinant acidic peptides designed based on a peptide extracted from an

exoskeleton of a crayfish on morphologies of the hybrids. Faraday Discuss. 2012;159:483–94.
8. Jono K, Nagao M, Oh T, Sonoda S, Hoshino Y, Miura Y. Controlling the lectin recognition of glycopolymers via distance arrangement of sugar blocks. Chem. Commun. 2018;54:82–5.
9. Danjo T, Enomoto Y, Shimada H, Nobukawa S, Yamaguchi M, Iwata T. Zero birefringence films of pullulan ester derivatives. Sci. Rep. 2017;7:46342.
10. Yan G, Yamaguchi T, Suzuki T, Yanaka S, Sato S, Fujita M, et al. Hyper-assembly of self-assembled glycoclusters mediated by specific carbohydrate-carbohydrate interactions. Chem Asian J. 2017;12:968–72.
11. Isogai A, Saito T, Fukuzumi H. TEMPO-oxidized cellulose nanofibers. Nanoscale. 2011;3:71–85.
12. Min BM, Lee SW, Lim JN, You Y, Lee TS, Kang PH, et al. Chitin and chitosan nanofibers: electrospinning of chitin and deacetylation of chitin nanofibers. Polymer. 2004;45:7137.
13. Sasaki Y, Akiyoshi K. Nanogel engineering for new nanobiomaterials: from chaperoning engineering to biomedical applications. Chem Rec. 2010;10:366–76.
14. Akiyoshi K Handbook of advanced glycoscience and glycoengineering. Tokyo: NTS; 2015.
15. Fujishiro T, Ogawa T, Matsuoka M, Nagahama K, Takeshima Y, Hagiwara H. Establishment of a pure culture of the hitherto uncultured unicellular cyanobacterium Aphanothece sacrum, and phylogenetic position of the organism. Appl Environ Microbiol. 2004;70:3338–45.
16. Okajima MK, Ono M, Kabata K, Kaneko T. Extraction of Novel Sulfated Polysaccharide from Aphanothece sacrum (Sur.) Okada, and its Spectroscopic Characterization. Pure Appl. Chem. 2007; 79:2039–46.
17. Okajima MK, Bamba T, Kaneso Y, Hirata K, Fukusaki E, Kajiyama S, et al. Supergiant ampholytic sugar chains with imbalanced charge ratio form saline ultra-absorbent hydrogels. Macromolecules. 2008;41:4061–4.
18. Okajima MK, Kaneko D, Mitsumata T, Kaneko T, Watanabe J. Cyanobacteria that produce megamolecules with efficient self-orientation. Macromolecules. 2009;42:3057–62.
19. Okajima MK, Miyazato S, Kaneko T. The cyanobacterial megamolecule sacran efficiently forms LC gels with very heavy metal ions. Langmuir. 2009;25:8526–31.
20. Okajima MK, Higashi T, Asakawa R, Mitsumata T, Kaneko D, Kaneko T, et al. Cyanobacterial polysaccharide gels with efficient rare-earth-metal sorption. Biomacromolecules. 2010;11:3172.
21. Okajima MK, Kumar A, Fujiwara A, Mitsumata T, Kaneko D, Ogawa T, et al. Anionic complexes of mwcnt with supergiant cyanobacterial polyanions. Biopolymers. 2013;99:1–9.
22. Mitsumata T, Miura T, Takahashi N, Kawai M, Okajima MK, Kaneko T. Ionic state and chain conformation for aqueous solutions of supergiant cyanobacterial polysaccharide. Phys Rev E. 2013;87:042607.
23. Okajima MK, Mishima R, Amornwachirabodee K, Mitsumata T, Okeyoshi K, Kaneko T. Anisotropic swelling in hydrogels formed by cooperatively aligned megamolecules. RSC Adv. 2015;5:86723–9.
24. Amornwachirabodee K, Okajima MK, Kaneko T. Uniaxial swelling in lc hydrogels formed by two-step cross-linking. Macromolecules. 2015;48:8615.
25. Okeyoshi K, Okajima MK, Kaneko T. Milliscale self-Integration of megamolecule biopolymers on a drying gas-aqueous liquid crystalline interface. Biomacromolecules. 2016;17:2096–103.
26. Shikinaka K, Okeyoshi K, Masunaga H, Okajima MK, Kaneko T. Solution structure of cyanobacterial polysaccharide, sacran. Polymer. 2016;99:767–70.
27. Joshi G, Okeyoshi K, Okajima MK, Kaneko T. Directional control of diffusion and swelling in megamolecular polysaccharide hydrogels. Soft Matter. 2016;12:5515–8.
28. Okeyoshi K, Okajima MK, Kaneko T. Emergence of polysaccharide membrane walls through macro-space partitioning via interfacial instability. Sci Rep. 2017;7:5615.
29. Okeyoshi K, Joshi G, Rawat S, Sornkamnerd S, Amornwachirabodee K, Okajima MK, et al. Drying-induced self-similar assembly of megamolecular polysaccharides through nano and submicron layering. Langmuir. 2017;33:4954–9.
30. Okeyoshi K, Osada K, Okajima MK, Kaneko T. Methods for self-integration of megamolecular biopolymers on the drying air-LC interface. J Vis Exp. 2017;122:e55274.
31. Okeyoshi K, Shinhama T, Budpud K, Joshi G, Okajima MK, Kaneko T. Micelle-mediated self-assembly of microfibers bridging millimeter-scale gap to form three-dimensional-ordered polysaccharide membranes. Langmuir. 2018;34:13965–70.
32. Okeyoshi K, Okajima MK, Kaneko T. Drying-induced macro-space partitioning of supra-polysaccharides and membrane formation with uniaxial orientation. Kobunshi Ronbunshu. 2018; 75:1–8.
33. Okeyoshi K. DRY & WET: in vitro dissipative structures of microtubules and polysaccharides by interfacial instability. Kobunshi Ronbunshu. 2018;75:396–405.
34. Okeyoshi K, Joshi G, Okajima MK, Kaneko T. Formation of polysaccharide membranes by splitting of evaporative air–LC interface. Adv Mater Interface. 2018;5:1701219.
35. Sornkamnerd S, Okajima MK, Kaneko T. Surface-selective control of cell-orientation on cyanobacterial liquid crystalline gels. ACS Omega. 2017;2:5304–14.
36. Sornkamnerd S, Okajima MK, Matsumura K, Kaneko T. Micropatterned cell orientation of cyanobacterial liquid-crystalline hydrogels. ACS Appl Mater Interfaces. 2018;10:44834–43.
37. Okajima MK, Sornkamnerd S, Kaneko T. Development of functional bionanocomposites using cyanobacterial polysaccharides. Chem Rec. 2018;167:1–12.
38. Yusof NFAA, Yamaki M, Kawai M, Okajima M, Kaneko T, Mitsumata T. Rheopectic behavior for aqueous solutions of megamolecular polysaccharide, sacran. Biomolecules. 2020; 10:155.
39. Budpud K, Okeyoshi K, Okajima MK, Kaneko T. Vapor-sensitive materials from polysaccharide fibers with self-assembling twisted microstructures. Small. 2020;16:2001993.
40. Okeyoshi K. DRY & WET: meniscus splitting from a mixture of polysaccharides and water. Polym J. 2020;52:1185–94.
41. De Gennes PG Scaling concepts in polymer physics. Ithaca, NY: Cornell, University Press; 1979.
42. Zhang YQ, Tanaka T, Shibayama M. Super-absorbency and phase transition of gels in physiological salt solutions. Nature. 1992;360:142.
43. Fraser JRE, Laurent TC, Laurent UBG. Hyaluronan: its nature, distribution, functions and turnover. J Intern Med. 1997;242:27.
44. Numata M, Asai M, Kaneko K, Bae AH, Hasegawa T, Sakurai K, et al. Inclusion of cut and as-grown single-walled carbon nanotubes in the helical superstructure of schizophyllan and Curdlan (β-1,3-glucans). J Am Chem Soc. 2005;127:5875–84.
45. Maurstad G, Danielsen S, Stokke BT. Analysis of compacted semiflexible polyanions visualized by atomic force microscopy: influence of chain stiffness on the porphologies of polyelectrolyte complexes. J Phys Chem B. 2003;107:8172–80.
46. Maurstad G, Stokke BT. Metastable and stable states of xanthan polyelectrolyte complexes studied by atomic force microscopy. Biopolymers. 2004;74:199–213.
47. Finlay IG, Mason MD, Shelley M. lancet Radioisotopes for the palliation of metastatic bone cancer: a systematic review. Oncol. 2005;6:392–400.

48. Wengler G, Wengler G, Koschinski A. A short treatment of cells with the lanthanide ions La^{3+}, Ce^{3+}, Pr^{3+} or Nd^{3+} changes the cellular chemistry into a state in which RNA replication of flaviviruses is specifically blocked without interference with host-cell multiplication. J Gen Virol. 2007;88: 3018–26.
49. De Gennes PG, Brochard-Wyart F, Quere D Capillarity and wetting phenomena: drops, bubbles, pearls, waves. New York, NY: Springer; 2003.
50. De Luca G, Rey AD. Monodomain and polydomain helicoids in chiral liquid-crystalline phases and their biological analogues. Eur Phys J E. 2003;12:291–302.
51. Liu J, Qi C, Tao K, Zhang J, Zhang J, Xu L, et al. Sericin/dextran injectable hydrogel as an optically trackable drug delivery system for malignant melanoma treatment. ACS Appl Mater Interfaces. 2016;8:6411–22.
52. Weaver CL, LaRosa JM, Luo X, Cui XT. Electrically controlled drug delivery from graphene oxide nanocomposite films. ACS Nano. 2014;8:1834–43.
53. Yuan X, Marcano DC, Shin CS, Hua X, Isenhart LC, Pflugfelder SC, et al. Ocular drug delivery nanowafer with enhanced therapeutic efficacy. ACS Nano. 2015;9:1749–58.
54. Li Z, Zheng Z, Su S, Yu L, Wang X. Preparation of a high-strength hydrogel with slidable and tunable potential functionalization sites. Macromolecules. 2016;49:373–86.
55. Zhao Y, Zhang Y, Liu A, Wei Z, Liu S. Construction of three-dimensional hemin-functionalized graphene hydrogel with high mechanical stability and adsorption capacity for enhancing photodegradation of methylene blue. ACS Appl MaterInterfaces. 2017;9:4006–14.
56. Liu H, Zuo K, Vecitis CD. Titanium dioxide-coated carbon nanotube network filter for rapid and effective arsenic sorption. Environ Sci Technol. 2014;48:13871–9.
57. Wang H, Zhang L, Li Y, Hu C. Influence of filtration aids on continuous filtration in membrane bioreactors. Ind Eng Chem Res. 2014;53:7202–8.
58. Brzoska JB, Brochard-Wyard F, Rondelez F. Exponential growth of fingering instabilities of spreading films under horizontal thermal gradients. Europhys Lett. 1992;19:97–102.
59. Shikinaka K, Okeyoshi K, Masunaga H, Okajima MK, Kaneko T. Structure of cyanobacterial polysaccharide, sacran. Polymer. 2017;99:767–70.
60. Zhao Y, Hien KTT, Mizutani G, Rutt HN, Amornwachirabodee K, Okajima MK, et al. Optical second-harmonic images of sacran megamolecules aggregates. J Opt Sci Am A. 2017;34:146.
61. Ngatu NR, Okajima MK, Yokogawa M, Hirota R, Eitoku M, Muzembo BA, et al. Anti-inflammatory effects of sacran, a novel polysaccharide from aphanothece sacrum,on 2,4,6-Trinitrochlorobenzene induced allergic dermatitis in vivo. Ann Aller Asthma Immunol. 2012;108:117.
62. Wathoni N, Motoyama K, Higashi T, Okajima MK, Kaneko T, Arima H. Physically crosslinked-sacran hydrogel films for wound dressing application. Int J Biol Macromol. 2016;89:465.
63. Fukushima S, Motoyama K, Tanida Y, Higashi T, Ishitsuka Y, Kondo Y, et al. Clinical evaluation of novel natural polysaccharides sacran as a skincare material for atopic dermatitis patients. J Cosm Derm Sci Appl. 2016;6:9–16.
64. Motoyama K, Tanida Y, Hata K, Hayashi T, AbuHashim II, Higashi T, et al. Cholesterol-lowering effect of Octaarginine-Appended β-Cyclodextrin in Npc1-Trap-CHO cells. Biol Pharma Bull. 2016;39:1172–8.
65. Fujishiro T, Ogawa T, Matsuoka M, Nagahama K, Takeshima Y, Hagiwara H. Establishment of a pure culture of the hitherto uncultured unicellular cyanobacterium Aphanothece sacrum, and phylogenetic position of the organism. Appl Environ Microbiol. 2004;70:3338.

Kosuke Okeyoshi is Associate Professor of Graduate School of Advanced Science and Technology, at Japan Advanced Institute of Science and Technology (JAIST). He received his Ph.D. in 2010 at The University of Tokyo. With the support of JSPS fellowships DC1, PD, and Research Abroad, he worked at The University of Tokyo, RIKEN, and Harvard University. Subsequently, he started working at JAIST from 2014 and his research interests focus on the design of biomimetic soft materials. To propose advanced energy converting systems, functional materials living within water are the target. Simultaneously, they are learning the laws of natural phenomena for the organization of polymer networks. He received the Award for Encouragement of Research in Polymer Science, The Society of Polymer Science, Japan in 2018.

Maiko K. Okajima who received Ph.D. from Tokyo Tech is a research fellow of the School of Materials Science at JAIST, Nomi, Japan, and R&D manager of Green Science Materials Inc. Japan. She has ~65 publications. She has been involved in industry-academic collaborative projects in the scientific fields of cyanobacteria, polysaccharides, biomedical design, etc. Additionally, she has engaged in establishment of start-up company on cyanobacterial polysaccharides and their applications as biomedical and cosmetic ingredients.

Tatsuo Kaneko received a B.S. and a Ph.D. in Polymer Chemistry from Tokyo Tech. One year before received Ph.D., he joined the faculty as an Assis Prof in the Department of Biology at Hokkaido University, and moved to Kagoshima University and Osaka University. After that, he joined the School of Materials Science at JAIST where he was promoted to Associate Professor and to Full Professor. He also joined the Bioengineering Department at UCLA as a Visiting Associate Professor. Current research interests include gels, soft matters, liquid crystals, polyelectrolytes, polypeptides, polysaccharides, and bio-derived/degradable plastics, for which he has received awards from Chemical Society of Japan and from several foundations. International prizes such as "Best presentation" at the 251st ACS National Meeting, "Distinguished Award" at the 12th IUPAC NMS-XII, "APSMR award" at the APSMR 2019 Annual Meeting, and "Gottfried Wagener prize" The 9th German Innovation Award have also been given.